

Conf - 830805 - -30

Thermo-structural and Thermal-hydraulic  
Aspects of the STARFIRE/DEMO Tritium Breeding Blanket\*

CONF-830805--30

DE83 010722

Y. Y. Liu, S. Majumdar, B. Misra

ARGONNE NATIONAL LABORATORY  
9700 South Cass Avenue  
Argonne, Illinois 60439

R. Burk and G. D. Morgan

MCDONNELL DOUGLAS ASTRONAUTICS COMPANY  
P. O. Box 516  
St. Louis, Missouri 63166

The submitted manuscript has been authored  
by a contractor of the U.S. Government  
under contract No. W-31-109-ENG-38.  
Accordingly, the U.S. Government retains a  
nonexclusive, royalty-free license to publish  
or reproduce the published form of this  
contribution, or allow others to do so, for  
U.S. Government purposes.

February, 1983

**DISCLAIMER**

This report was prepared as an account of work sponsored by an agency of the United States Government. Neither the United States Government nor any agency thereof, nor any of their employees, makes any warranty, express or implied, or assumes any legal liability or responsibility for the accuracy, completeness, or usefulness of any information, apparatus, product, or process disclosed, or represents that its use would not infringe privately owned rights. Reference herein to any specific commercial product, process, or service by trade name, trademark, manufacturer, or otherwise does not necessarily constitute or imply its endorsement, recommendation, or favoring by the United States Government or any agency thereof. The views and opinions of authors expressed herein do not necessarily state or reflect those of the United States Government or any agency thereof.

MASTER

7/18

DISTRIBUTION OF THIS DOCUMENT IS UNLIMITED

\* Work supported by the U.S. Department of Energy.

INVITED lecture to be presented at the 7th International Conference on  
Structural Mechanics in Reactor Technology, Chicago, IL, August 22-26, 1983.

### Abstract

The STARFIRE/DEMO Project has performed a conceptual design study of the demonstration fusion power reactor to follow the FED/INTOR class of experimental tokamaks. This paper discusses thermo-structural and thermal-hydraulic aspects of two fundamentally different first wall and tritium breeding blanket concepts for STARFIRE/DEMO. The first concept uses solid lithium oxide ( $Li_2O$ ) as the tritium breeder in a modular blanket. The first wall is a flat corrugated panel. Both first wall and blanket are constructed of titanium-modified austenitic stainless steel and are cooled with pressurized high-temperature water. The second concept features a liquid metal, 17Li-83Pb, as tritium breeder and coolant. The blanket module's two semi-cylindrical front walls form the first wall, the back faces of which are cooled by flowing liquid metal. Ferritic steel and vanadium alloy are the candidate structural materials.

Thermal-hydraulic analyses were performed for the solid-breeder blanket to investigate the sensitivity of breeder temperatures to variations in physical parameters (i.e., thermal conductivity and interface thermal conductance) and fluctuations in power level. The study is important to assure that breeder temperatures stay within the allowable limits during blanket operation.

Thermoelastic stress analyses of the  $Li_2O$  breeder were conducted using a simple cylindrical model to determine the breeder's propensity to fracture under operational thermal gradients (410°C to 660°C outward radially from the cylinder's central coolant tube, over a 2 to 6 cm thickness). The analyses indicate high propensity for radial and axial crack formation and several remedies are being considered to alleviate the cracking problem.

Primary and secondary stress calculations for four different first wall/coolant channel configurations of the solid-breeder blanket were performed to determine their structural requirements (i.e., thickness). Channels with cross sections bounded by semicircular arcs in the corrugated sheet exhibited lower thermal and mechanical stress levels than arc segments or sinusoidal shapes.

Thermal-hydraulic analyses were performed for the liquid-breeder blanket to investigate the sensitivity of structural material temperatures to variations in the structural thickness and coolant velocity (or channel width). The results showed that the maximum allowable temperature for structural materials sets the design limit; no other problems were anticipated.

Elastic- and thermal-stress analyses were performed for the liquid-breeder blanket to determine its structural requirements (i.e., thickness and internal frame spacing). Plastic analyses will be required for future analytical refinement.

## 1. Introduction

The STARFIRE/DEMO Project has performed a conceptual design study of a demonstration fusion power reactor to follow the Fusion Engineering Device (FED)/International Tokamak Reactor (INTOR) class of experimental tokamaks. Two fundamentally different DEMO first wall and tritium-breeding blanket concepts were considered. The first concept uses solid lithium oxide ( $Li_2O$ ) as the tritium breeder in a modular blanket. The first wall is a flat corrugated panel. Both first wall and blanket structural materials are constructed of titanium-modified austenitic stainless steel and are cooled with pressurized high-temperature water. The second concept features a liquid metal,  $17Li-83Pb$  (subsequently referred to as Li-Pb), as tritium breeder and coolant. Two semi-cylindrical front walls of the blanket module form the first wall and their back faces are cooled by flowing liquid metal. Ferritic steel (HT-9) and vanadium alloy (V-15Cr-5Ti) are the candidate structural materials.

This paper describes the design features and presents highlights of the thermal-hydraulic and thermo-structural analyses of the two blanket concepts. Detailed results and discussions of this work will be published elsewhere [1, 2].

## 2. Solid Breeder Blanket Concept

### 2.1 Design Features

The DEMO reference first wall/solid-breeder blanket design concept is illustrated schematically in Fig. 1. Selected materials, design options, and major operating parameters are listed in Table I.

The reference blanket design uses the concept of individual first wall/blanket modules configured as parallelepipeds. These modules are assembled into sectors. Eight of these sectors, identical except for local modifications (e.g., to accommodate REB diode leads), comprise the reactor first wall/blanket system.

The first wall (shown in Fig. 1) is an actively cooled panel made of Prime Candidate Alloy (PCA), a titanium-modified advanced austenitic stainless steel. The cooled structural panel is continuous down both sides of the modules to the rear of the breeding zone. The inlet and outlet ends of the panel terminate in headers in the manifold zone. The first wall is mechanically and structurally integrated with the blanket. Actively cooled support frames within the breeding zone are welded to the back side of the first wall and to the rear wall of the breeding zone to provide structural rigidity and to avoid flow-induced vibration.

The  $Li_2O$  breeder is contained within the boundary formed by the six sides of the module. The toroidally-oriented coolant tubes in the breeder zone are arrayed in banks; each tube makes a single pass through the breeder. Tube spacing radially and poloidally through the breeding zone is graded in proportion to the local nuclear heating rate, to ensure that the breeder is maintained within the design-basis minimum and maximum temperature limits of  $410^\circ C$  and  $660^\circ C$ , respectively, at all points. For each tube, coolant temperature is

increased from 260°C at the inlet to 300°C at the outlet by orificing at the tube entrance to produce the proper flow rate.

Helium purge gas is used to remove tritium from the breeder. The low pressure (~ 1 atm), low flow-rate gas is introduced into the pressure-tight breeding zone at one end of the module through the rear wall. The gas flows in the toroidal direction through narrow channels (~ 2 mm dia.) pre-formed in the breeder, and exits through the rear wall at the other end of the module. The  $\text{Li}_2\text{O}$  breeder is fabricated in the form of sintered or hot

pressed blocks having 30% porosity, which are fitted around the U-bend tubes during assembly of the blanket. The configuration and the assembly method of the blocks necessary to accommodate thermal-stress-induced cracking must be determined through future development efforts.

## 2.2 Thermal-hydraulic Analysis

Parametric studies were carried out to determine the changes in breeder temperatures with variations in such key physical parameters as breeder thermal conductivity ( $k_B$ ), breeder-to-coolant-tube interface thermal conductance ( $h_I$ ), and blanket operating parameters such as reactor power level. The results of these studies, and their implications for the reference blanket design, are discussed in this section.

The one-dimensional (1-D) cylindrical blanket-cell model shown schematically in Fig. 2a was used for most of the scoping studies. Although the temperature distribution in the breeding blanket is three-dimensional, the cylindrical blanket cell model permits mathematical simplifications. The assumptions of uniform internal heat generation and temperature-independent material and fluid properties permit the governing equations to be solved in closed form, greatly facilitating parametric investigations. Reference geometric and operating parameters used for the sensitivity study are those given in Table I. Three blanket regions, each representative of a blanket region away from the plasma side, were chosen for investigation. Region 1 was taken near the first wall and has the maximum nuclear heating rate of 12.94 W/cc. Region 2 was taken within the breeder zone where the nuclear heating rate is  $\sim 25\%$  of that in Region 1. Region 3 was taken near the reflector/shield where the nuclear heating rate is  $\sim 4\%$  of that in Region 1. For each region, a constant zone-averaged nuclear heating rate was used.

Table II summarizes the results of the sensitivity studies. Breeder temperatures are found to be sensitive to each of the parameters, and the degree of sensitivity to each is comparable. In some cases ( $k_B$  for example), the range considered for variation is believed reasonable, taking into account the irradiation degradation effects on  $k_B$ . In other cases, ( $h_I$  for example), the range considered for variation may involve larger uncertainty than that for  $k_B$ .

One might ask why it is so important to stay within the maximum and the minimum temperatures. These temperature bounds are imposed from considerations of both tritium release and microstructural stability. For  $\text{Li}_2\text{O}$  in particular, the lower temperature bound (410°C) is set to ensure adequate solid-state tritium diffusion and to avoid LiOT liquid-phase formation which may seal off the interconnected porosity path for tritium release. The upper temperature bound (660°C) is set to prevent high-temperature sintering and grain growth.

### **2.3 Thermo-structural Analysis**

#### **A. Solid Breeder Physical Integrity**

Maintaining  $\text{Li}_2\text{O}$  breeder temperatures during blanket operation within the limits established by materials considerations is considered to be the key to successful tritium recovery. Previous design calculations showed that the minimum and maximum  $\text{Li}_2\text{O}$  temperature requirements can be satisfied by proper selection of coolant conditions, tube dimensions, and tube spacing. Results in Sec. 2.2, however, also illustrated the important role of breeder-

to-tube interface thermal conductance, and of breeder thermal conductivity, on breeder temperatures. All of these calculations were made assuming that  $\text{Li}_2\text{O}$  remains intact (i.e., a sintered solid) and retains its as-fabricated configuration during operation. An assessment was made of  $\text{Li}_2\text{O}$  integrity under DEMO blanket steady-state operating conditions. The assessment, which focused specifically on the thermoelastic response of  $\text{Li}_2\text{O}$  under thermal gradients, is presented below.

For analytical simplicity, the  $\text{Li}_2\text{O}$  solid breeder was represented either by a thick, hollow cylinder, or by a thin disc with a central hole. Except for the region involving the coolant tube, the models are identical to the cylindrical cell model used in the blanket thermal hydraulic study (Fig. 2a). Simplifying assumptions of axisymmetry and temperature-independent material properties were made and standard formulae [3] were used for the principal thermoelastic stress components under conditions of either generalized plane strain (for the thick, hollow cylinder) or plane stress (for the thin disc).

Figure 3 shows the calculated temperatures and stresses in Region 1 of the thick cylinder; results are similar for Regions 2 and 3. Of the three principal stresses in each blanket region,  $\sigma_\theta$  and  $\sigma_z$  are both tensile near the breeder-to-tube interface, and compressive near the cell outer boundary. Maximum tensile stresses occur at  $r = a$  where  $\sigma_\theta = \sigma_z$ . If the maximum tensile principal stress is used as a fracture criterion for  $\text{Li}_2\text{O}$ , one can expect equal likelihood for  $\sigma_\theta$ -induced (radial) and  $\sigma_z$ -induced (axial) cracks to form first from the breeder-to-tube interface. In view of the relatively low flexural strength reported [4] for  $\text{Li}_2\text{O}$  (i.e.,  $\sigma_f = 48.3$  MPa), the cracking tendency appears very high since the maximum tensile stresses, 1076.9, 1131.3, and 1203.1 MPa for Regions 1, 2, 3, respectively, have all greatly exceeded the flexural strength.

For the  $\text{Li}_2\text{O}$  solid breeder dimensional change, the contribution to the gap-size change at the breeder-to-tube interface from  $\text{Li}_2\text{O}$  thermal expansion is an increase of  $\sim 0.12$  mm. The axial thermal expansion strains are  $\sim 1.8\%$ . If the breeder length is taken to be the same as the blanket coolant channel length of 3 m, the axial thermal expansion of the breeder will be  $\sim 54$  mm. These thermal expansion values give a crude indication of the breeder dimensional change.

For the thin-disc model, the maximum tensile stresses can be readily obtained from the thick-cylinder solution. One needs only to multiply  $\sigma_r$  and  $\sigma_\theta$  in Fig. 3 by a factor of  $(1 - v)$  to obtain the plane-stress results. With  $v = 0.3$ , the maximum tensile circumferential stresses ( $\sigma_\theta$ ) in the thin disc are, therefore, 753.8, 791.9, and 842.2 MPa for Regions 1, 2, and 3, respectively. Since all these stresses are still much higher than the flexural strength of  $\text{Li}_2\text{O}$ , the tendency for the formation of  $\sigma_\theta$ -induced radial cracks in thin-disc  $\text{Li}_2\text{O}$  remains high, even though axial crack formation is prevented because  $\sigma_z$  is very small. Notice also that even though  $\sigma_r$  in Fig. 3 is greater than  $\sigma_f$ , the  $\sigma_r$ -induced (circumferential) cracks are unlikely to form compared to the much higher propensity for the formation of radial and axial cracks. Once those cracks form, stress redistribution occurs, and the stress patterns are no longer given by those in Fig. 3.

Breeder cracking, if it occurs, will change the blanket configuration and increase the difficulty in predicting and controlling breeder performance during operation. For example, the effects of a gap size change due to  $\text{Li}_2\text{O}$  thermal expansion at the breeder/tube interface must be accounted for in thermal conductance calculations. The cracks themselves, if

unfavorably oriented, can increase the impedance to heat flow and thereby violate the breeder maximum temperature limit. In the  $\text{Li}_2\text{O}$  reference blanket design concept, the primary heat flow is in the radial direction, and the formation of circumferential ( $\sigma_r$ -induced) cracks to impede radial heat flow is least likely. Radial and axial cracks, on the other hand, do not represent barriers for radial heat conduction, even though the local temperatures will be influenced by the heat-transfer medium (helium purge gas) between the crack faces. The creation of new surfaces should also aid tritium release by reducing the diffusion path.

It is for these reasons that the DEMO project is considering using metallurgical bonds and a closely-controlled conducting medium instead of a helium gap. Segmentation of the breeder cylinder, both axially and circumferentially, to relieve thermal stresses to levels below the fracture strength of  $\text{Li}_2\text{O}$  is also being considered. High fabrication and assembly costs, as well as other difficulties may arise with the above approach, and alternative designs are being contemplated.

### B. First Wall Stress Analysis

An important aspect of the first wall design with pressurized water coolant is the coolant channel configuration. Four options have been analyzed for stresses: (1) a grooved channel in the back of the first wall, covered with a flat plate, (2) a solid first wall with a corrugated panel in the shape of a sine wave, (3) a solid first wall with a corrugated panel in the shape of an arc of a circle, and (4) a solid first wall with a corrugated panel in the shape of a semi-circle.

The four configurations are compared for the same width (W). The sinusoidal panel and the circular arc panel are compared for the same width to height (W/h) ratio. Primary and secondary stresses from mechanical and thermal loading were determined, and the results are summarized below.

The maximum primary stress intensity ( $P_m$ ) is plotted in Fig. 4a as a function of the panel wall thickness, for unit pressure, at a W/h value of 4. The maximum stress intensity at any point is defined by twice the maximum shear stress at that point. The lowest primary membrane stress occurs for the semicircular case. For widths greater than 10 mm and thicknesses less than 4 mm, the primary membrane stress in the circular arc is less than that in either the flat plate or the sinusoidal panel. For lesser widths ( $W = 5$  mm) the differences among the four geometries are small. Since the DEMO maximum coolant pressure (P) is 11 MPa, the primary membrane stresses are small compared to the allowable values, particularly for channel widths  $\leq 10$  mm; and the primary stress intensities are less than the allowable  $S_m$  values for either annealed or cold-worked (CW) Type 316 SS.

Figure 4b is a plot of the maximum primary local membrane plus bending stresses. For small channel widths ( $\sim 5$  mm) both the flat plate and the sinusoidal panel have the lowest stress; however, the differences among the four geometries are not large. For larger channel widths and smaller thicknesses, bending effects are dominant, and the semicircular panel exhibits the lowest stress intensity and the flat plate the highest stress intensity. For the 5 mm channel width, all four geometries satisfy the  $1.5 S_m$  requirement for either annealed or CW Type 316 SS for all thicknesses considered. The same is true for 10 mm channel widths, provided the front plate thickness is greater than 2.5 mm.

Figure 4c shows the variation of maximum thermal stress for different  $\Delta T$  between the average temperature of the first wall and the rear panel. The semicircular panel provides

the lowest stress. The circular arc panel experiences the largest thermal stress, which occurs at the attachments to the first wall due to bending. Figure 4d shows the total primary plus secondary stress for panels of 10 mm channel width, for  $\Delta T = 50^\circ\text{C}$  and  $100^\circ\text{C}$ . The figure also shows the allowable  $3 S_m$  limits (dashed line) for both annealed and CW Type 316 SS. The CW material is acceptable for all geometries at both  $\Delta T$  values. The annealed material is acceptable only for the semicircular panel at  $\Delta T = 100^\circ\text{C}$ , but for  $\Delta T = 50^\circ\text{C}$  the flat plate and sinusoidal panels also satisfy the  $3 S_m$  limit.

From the viewpoint of stress, the semicircular panel configuration is the most desirable. However, considerations of cooling efficiency and of fabrication cost might indicate the circular arc or sinusoidal configuration to be a better choice. Further analyses should also be performed to determine the stress effects of using relatively thin front plates. These would be permitted by the very low particle flux to most of the first wall for the DEMO reactor.

### 3. Liquid Breeder Blanket Concept

#### 3.1 Design Features

The DEMO reference first wall/liquid-breeder blanket design concept is illustrated schematically in Fig. 5. Geometry, materials and operating parameters are given in Table III. The reference blanket design uses the concept of integral first wall/blanket modules configured as double-headed, elongated radial-flow cells, similar to the STARFIRE backup design using liquid lithium [5]. The walls of the plasma side of the flow cell constitute the first wall and both ferritic steel (HT-9) and a vanadium alloy (V-15Cr-5Ti) are being considered as the structural materials. The semi-cylindrical heads are cooled from the backside by flowing Li-Pb, which serves both as the breeder and the coolant. The Li-Pb enters the blanket through a standpipe, flows from a manifold through the gap between a baffle and the first wall, then reenters the chamber from which it is withdrawn through holes in the rear wall of the cells. This concept minimizes voids in the regions which are available for breeding, and also minimizes associated neutron streaming problems. This helps to assure that the STARFIRE/DEMO blanket would produce a net breeding ratio  $> 1$  in actual practice. The module walls are pressurized internally to  $\sim 1\text{-}2$  MPa, however, owing to (1) the interconnection of the blanket modules combined with the high density of the Li-Pb, and (2) the pressure head required to pump the Li-Pb through the primary coolant system. This requires internal frames spaced relatively close together to break up the large-area flat walls into smaller panels.

### 3.2 Thermal Hydraulic Analysis

A preliminary thermal hydraulic analysis was performed for the Li-Pb self-cooled blanket concept described in Sec. 3.1, in order to determine the temperature distributions in the first wall/coolant channel region of the blanket. For the analysis, the parameters of coolant channel width, first wall thickness, coolant temperature increase (inlet to outlet for the blanket), and module semi-cylindrical head diameter were varied to investigate a range of allowable values. The resulting temperature distributions were later used as input to the thermo-structural analysis described in Sec. 3.3.

Figure 6 shows the model for the thermal hydraulic calculations. In this model, it is assumed that the first wall has a beryllium coating for plasma impurity control. The

calculations are based on the information given in Table IV, with assumed nuclear heating rates of 11.5, 22.2, and 11.27 W/cc, respectively, for the structural material, breeder/coolant, and Be coating.

The surface heat flux on the first wall (diameter = 30 cm) is assumed to have a  $\cos \phi$  distribution ( $\phi$  = angle away from the point closest to the plasma). Assuming uniform flux distribution in the lengthwise (toroidal) direction of the blanket modules, one can perform the thermal analysis based on two-dimensional heat conduction. The module was divided into ten regions in the  $\theta$ -direction, two regions in the Be coating, and three regions in the plate (all in the radial direction). The baffle plate between the first wall and the blanket region is assumed to be perforated to prevent stagnant thermal regions behind the baffle. Nominal thicknesses of the Be coating, first wall, coolant channel, and baffle plate were all taken to be 3 mm. To simplify the calculations, thermal interactions between the first wall region and other regions are assumed to be negligible.

Table IV summarizes the results of the parametric studies. For the reference case, the maximum surface temperatures in HT-9 and the beryllium coating occur just past the head centerline and are 414 and 480°C, respectively. These temperatures vary with structural thickness and channel width (or coolant velocity). For the cases included in the analyses, the coolant outlet temperature appears to set the upper temperature limit for the structural material.

If 450°C is assumed to be the upper temperature limit for HT-9, then the coolant temperature rise would be limited to 150°C. For the vanadium alloy, the allowable coolant temperature rise may be as high as 200°C. This provides additional flexibility in the blanket design. The thickness of the Be coating was assumed to be 3 mm, which resulted in a maximum temperature of 480°C for the reference case. On the basis of temperature alone, thicker coatings can be used, if necessary, for plasma impurity control; however, stress analyses should be carried out to determine maximum allowable coating thicknesses.

### 3.3 Stress Analysis of Li-Pb Self-Cooled Blanket Module

To determine the structural requirements for the double-head module concept described in Sec. 3.1, a preliminary stress analysis was performed for a typical blanket module. The required structural arrangement, thicknesses, and allowable relationships among the various design parameters were studied. Coolant pressure was assumed to be 1.4 MPa (including pumping head pressure). Temperature distributions from the thermal-hydraulic analysis of Sec. 3.2 were used to determine thermal stresses. Allowable stresses for both HT-9 ferritic steel and vanadium alloy were based on the ASME Boiler Code Section III, Division I, Class 2. This defines (1) an allowable stress for primary loads (pressure in this instance) of  $1.5 S_m = 1.5 (F_{tu}/3) = F_{tu}/2$ , and (2) an allowable stress for primary plus secondary loads (thermal stresses in this instance) as  $3 S_m = 3 (F_{tu}/3) = F_{tu}$ , where  $F_{tu}$  is the allowable stress for HT-9 at 450°C taken to be 525 MPa. As a simplification for this analysis, the latter limit was taken as  $1.5 S_m$  for primary stresses and  $1.5 S_m$  for secondary stresses.

Only elastic analysis was performed. Since the limit ( $F_{tu}$ ) for primary and secondary stresses is above the yield stress, significant plasticity can occur during operational cycling (due to plasma disruptions) of pressures and temperatures. The elastic analysis described here is thus only a first approximation to determine the structural requirements; future effort should include plastic analysis, particularly for lifetime estimation.

The module structural configurations are shown in Fig. 7. Dimensions shown are for the

HT-9 ferritic steel. The 1.4 MPa internal pressure acts on the side walls which beams this load to the internal frames. Loads on the side walls for vertically oriented modules are equal and are self-reacted through the frames. Differences in side wall loads for other modules due to the internal static head difference and breeder gravity loads are reacted by the side wall to the frames. The frames, in turn, react these loads in shear to the back wall. Even though the side walls are cylindrical in the first wall section, the principal load path in the skin for internal pressure is still in the toroidal direction, as the skin beams the pressure to the tension webs. In the present module design, the hoop tension path in the poloidal direction does not have a rigid support at the cusp between heads on the module center line, and hence is only partially effective. Accordingly, this analysis conservatively excludes the hoop tension load path.

It is desirable to minimize the structural volume of the blanket module to provide as large a breeder/coolant volume fraction as possible. Considering only the side walls (sized by pressure), and minimum gage internal frames (1-mm thick plus 25% for stiffeners), a minimum structural volume condition for HT-9 was found at a spacing of 8 cm, as shown in Fig. 8. Although this provides a rationale for selecting a frame spacing and wall thickness, other criteria (e.g., maximizing coolant temperature rise) modified this solution to a 5.7 cm spacing (still near minimum structural volume fraction).

Thermal stresses were calculated for the temperature conditions given in Sec. 3.2. They consist of two parts: (1) a local thermal stress ( $\sigma_{t1}$ ) due to temperature variation through the wall thickness; and (2) overall thermal stress ( $\sigma_{t0}$ ) due to temperature variation on the blanket cross section (stress in toroidal direction). Temperature variation through the thickness is almost linear, and a simple plate relationship was used for a first estimate. The baseline configuration analyzed has a  $\Delta T$  through the thickness of 62.8°C. This results in a local thermal stress for HT-9 of 94.6 MPa. This is about a third of the assumed allowable secondary stress (1.5  $S_m$ ). In a blanket sector, adjoining modules may act near-adiabatically so that through-thickness  $\Delta T$  values in the side walls (and thus the related thermal stresses) will be negligible.

Overall thermal stresses were elastically calculated for the blanket module cross-section. The analysis assumes the blanket module is unconstrained either in axial extension or in bending (e.g., a "free" beam). The maximum overall thermal stress (151 MPa) occurs in the cusp area on the inboard wall. This represents about 2/3 of the assumed allowable secondary stress (1.5  $S_m$ ).

Temperatures for the first wall region of the module were calculated as discussed in Sec. 3.2 for different values of side wall thickness ( $t_w$ ), coolant channel thickness ( $t_c$ ), cylinder diameter (D), and coolant temperature rise ( $T_c$ ). Temperatures for the flat portions of the side walls were calculated by linearly interpolating between the temperature of the last element in the first wall and the assumed coolant outlet temperature. The effects of using both the HT-9 ferritic steel and vanadium alloy were evaluated. The effects of these variations (taken one at a time) on thermal stresses and allowables were calculated using linear approximations. By adding these sensitivities together and curve fitting through the baseline thermal stress, a linear equation for thermal stress was obtained as a function of the parameters  $t_w$ ,  $t_c$ ,  $T_c$ , and D. A similar equation was generated for the average temperature of the highest temperature element in the front wall region as a function of the

same parameters. Since the allowable stress for a material is a function of temperature, the allowable stress was then known as a function of the other parameters. By equating allowable stress to the calculated thermal stress, a relationship was obtained among the parameters that would not over-stress the first wall. This relationship is shown in Fig. 9 for both HT-9 and V-15Cr-5Ti. To maximize the allowable coolant temperature rise, it is desirable to minimize the wall thickness and half-cylinder diameter, and to a lesser extent to minimize the thickness of the first wall coolant channel. The vanadium alloy can be used at higher temperatures than HT-9 because it has a higher allowable stress and lower thermal stress. Thus the vanadium alloy can be used with a significantly higher coolant temperature rise (and hence a higher energy conversion efficiency) for a given wall thickness, as is evident from inspection of Fig. 9.

In summary, the module configuration using either HT-9 ferritic steel or V-15Cr-5Ti alloy appears adequate to provide sufficient strength for the assumed pressures and coolant temperatures. However, the structure is complicated by the internal frames which are necessary to react pressure loads on the flat side walls. This may make the structure more difficult and expensive to fabricate. Use of the V-15Cr-5Ti alloy allows increased cooling efficiency, or a reduction in the number of internal frames, due to its better mechanical and thermal properties.

#### 4. Summary

Design features, thermal-hydraulic and thermo-structural aspects of the STARFIRE/DEMO tritium breeding blanket have been described for two fundamentally different concepts: 1) solid  $\text{Li}_2\text{O}$  breeder/pressurized  $\text{H}_2\text{O}$  coolant/Ti-modified austenitic stainless steel, and 2) self-cooled 17Li-83Pb liquid breeder/coolant/ferritic steel or vanadium alloy. First-order thermal hydraulic and thermo-structural analyses were performed for initial design calculations which showed favorable results for the viability of each concept as well as problematic areas requiring further investigation.

#### References

- [1] LIU, Y. Y., et al., to be published in Nucl. Engng. & Design.
- [2] ABDOU, M. A., et al., "A Demonstration Tokamak Power Plant Study (DEMO)," ANL/FPP-82-1 (1982).
- [3] BOLEY, B. A., and WEINER, J. H., Theory of Thermal Stresses, John Wiley & Sons, 1960, p. 290.
- [4] KOENIG, J. H., Rutgers University, Ceram. Res. Sta. Prog. Rprt. 2 (1953).
- [5] BAKER, C. C., et al., ANL/FPP-80-1 (1980).

List of Tables

- I. DEMO Reference First Wall/Blanket Concept Description (Solid Breeder).
- II. Li<sub>2</sub>O Solid Breeder Temperature Sensitivity to Variations of  $k_B$ ,  $h_I$  and Power Level Q.
- III. DEMO Reference First Wall/Blanket Concept Description (Liquid-metal Breeder).
- IV. Li-Pb Liquid Breeder First Wall Temperature Sensitivity to Variations of Structural Thickness and Coolant Velocity (or Channel Width).

Table I. DEMO Reference First Wall/Blanket Concept Description  
(Solid Breeder)

---

Selected Materials

- Tritium Breeder	$\text{Li}_2\text{O}$ (solid; 70% dense)
- Coolant	Pressurized $\text{H}_2\text{O}$
- Tritium Processing Fluid	Low-velocity Helium (0.05 MPa)
- Structure	Titanium-modified Austenitic Stainless Steel

Selected Design Options

- First Wall	Be-clad Corrugated Panel	
- Breeder Coolant Containment	Small-diameter Tubes	
- Other	<ul style="list-style-type: none"><li>- First wall and blanket mechanically and structurally integrated</li><li>- Coolant flow in toroidal direction</li><li>- Dual parallel primary coolant loops</li><li>- Maintenance by sector removal and replacement</li></ul>	
<hr/>		

Operating Parameters

- Maximum Allowable Temperature	660°C
- Minimum Allowable Temperature	410°C
- Coolant Inlet Temperature	260°C
- Coolant Outlet Temperature	300°C
- Coolant Pressure	11.0 MPa
- Integrated Neutral Wall Load (Average)	1.8 MW/m <sup>2</sup>

---

Table II.  $\text{Li}_2\text{O}$  Solid Breeder Temperature Sensitivity to Variations of  $k_B$ ,  $h_I$ , and Power Level Q

	$T_{\max}$ ( $^{\circ}\text{C}$ )	$\Delta T$ ( $^{\circ}\text{C}$ )*	$T_{\min}$ ( $^{\circ}\text{C}$ )	$\Delta T$ ( $^{\circ}\text{C}$ )*
Reference Case	660	--	410	--
$k_B$ (+ 10%)	637	-23	410	--
$k_B$ (- 10%)	688	28	410	--
$k_B$ (- 67%)	1168	508	410	--
$h_I$ (+ 22%)	644	-16	394	-16
$h_I$ (- 18%)	680	20	430	20
Q (+ 10%)	709	49	421	11
Q (- 10%)	612	-48	393	-17

$\Delta T$  = difference between the new temperature (maximum or minimum) calculated with parameter variation and the reference temperature (maximum or minimum).

Table III. DEMO Reference First Wall/Blanket Concept Description  
(Liquid-metal Breeder)

---

Selected Materials

- Tritium Breeder	17Li-83Pb (liquid)
- Coolant	17Li-83Pb (liquid)
- Structure	Ferritic Steel (HT-9) Vanadium Alloy (V-15Cr-5Ti)

Selected Design Options

- First Wall	Be-clad, Double-headed Semi-cylindrical Cell
- Breeder Coolant Containment	Elongated Flow Cells
- Other	
- Integral first wall and blanket	
- Coolant in radial direction	
- Maintenance by sector removal and replacement	

Operating Parameters

- Coolant Inlet Temperature	300°C
- Coolant Outlet Temperature	450°C
- Surface Heat Flux Wall Load	0.5 MW/m <sup>2</sup>
- Coolant Pressure	1.4 MPa

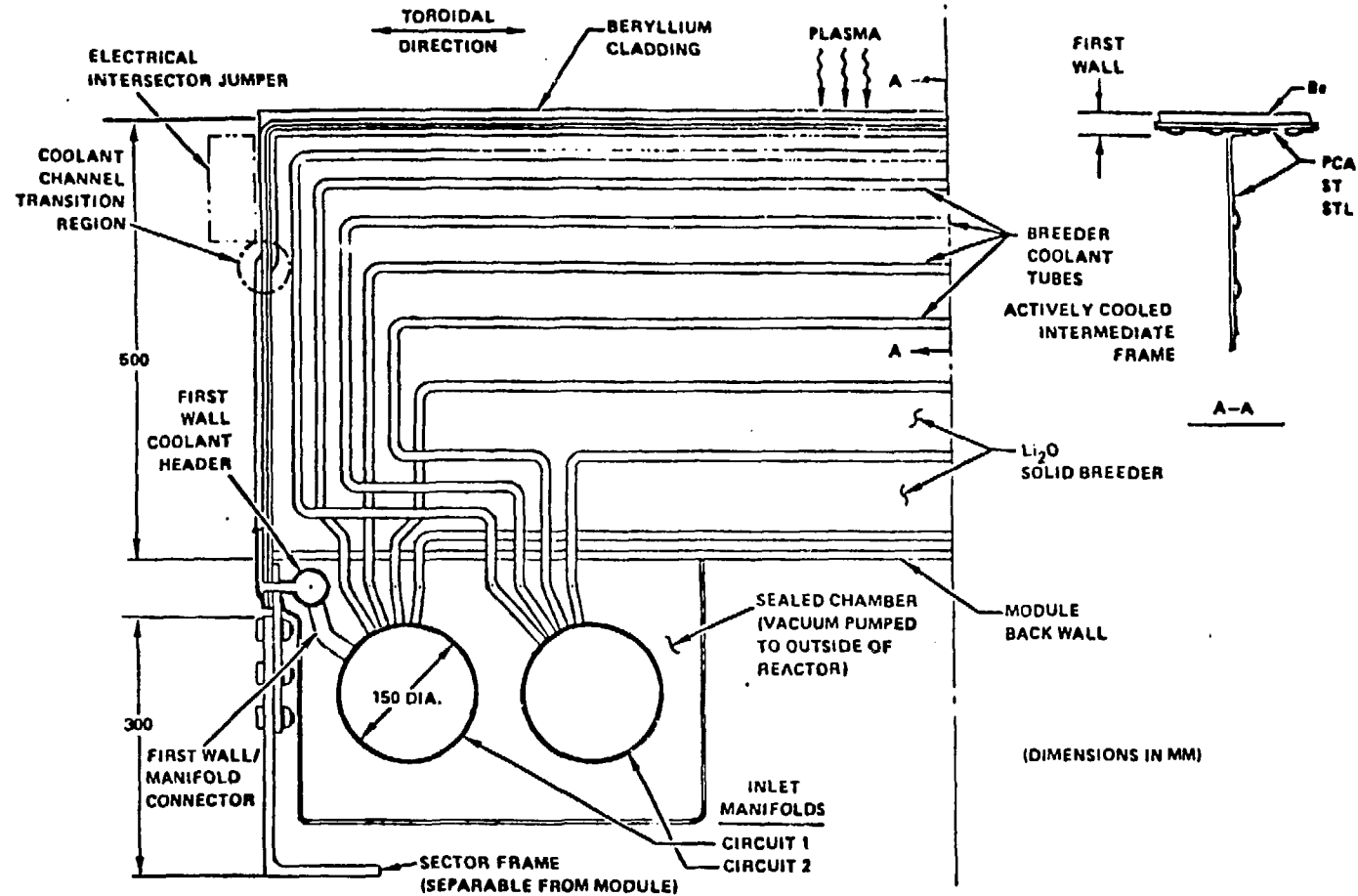
---

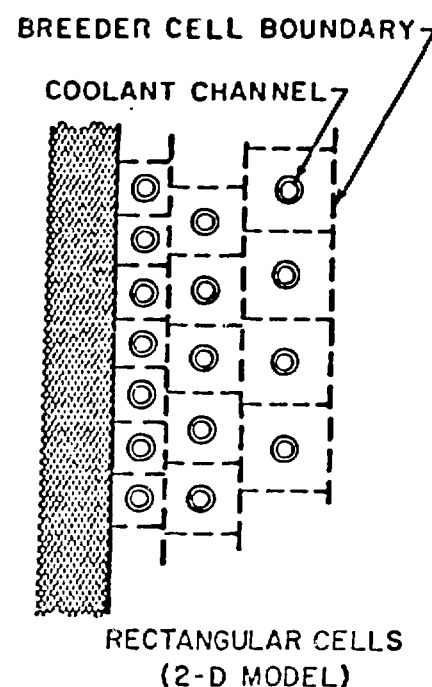
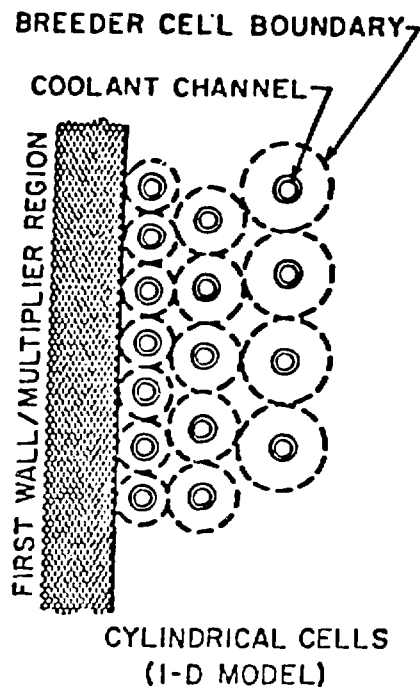
**Table IV. Li-Pb Liquid Breeder First Wall Temperature Sensitivity to Variations of Structural Thickness and Coolant Velocity (or Channel Width)**

	Structural	$T_{max}$ (°C)	Be-Coating
Reference Case (HT-9)	414		480
Structural Thickness, + 50%	446		513
Coolant Velocity, - 33%	425		493
- 50%	436		504
- 70%	467		535

List of Figures

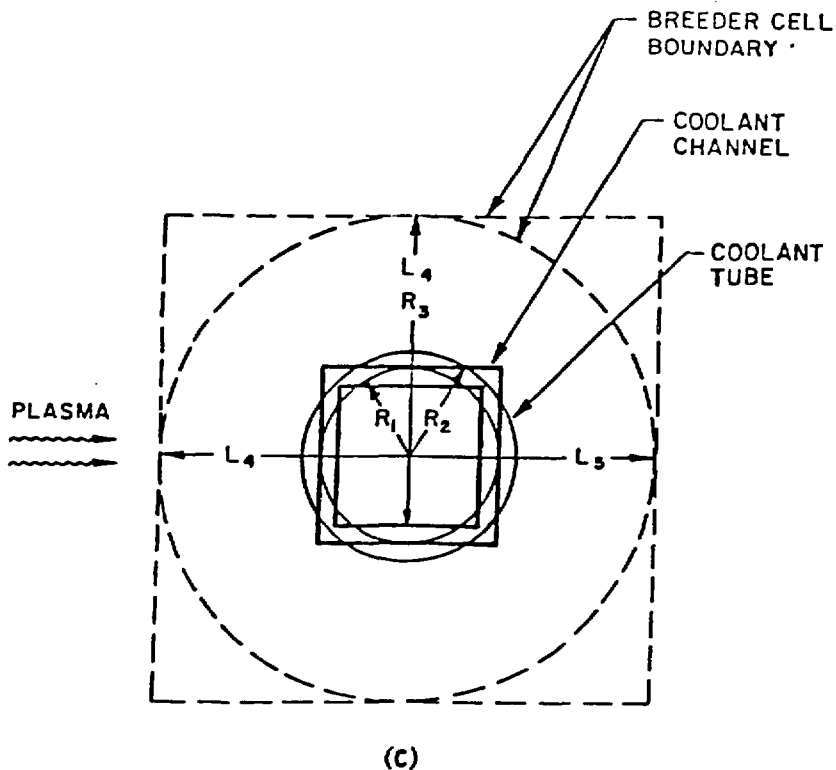
1. DEMO  $\text{Li}_2\text{O}$  solid breeder blanket concept.
2. Schematics of cylindrical and rectangular blanket cell models.
3. Calculated radial temperature and thermoelastic stress distribution in Region 1 of the blanket (thick, hollow-cylinder model).
4. (a) Maximum primary membrane stress intensities.  
(b) Maximum primary membrane local plus bending stress intensities.  
(c) Thermal stresses.  
(d) Maximum primary local membrane plus bending plus secondary stress and 3  $S_m$  allowable stresses.
5. DEMO liquid breeder blanket concept.
6. Liquid breeder blanket thermal-hydraulic model showing distribution of node points.
7. Structural sizing for Li-Pb self-cooled blanket concept.
8. Frame spacing in Li-Pb self-cooled blanket for minimum structural volume.
9. Allowable relationships of blanket parameters.

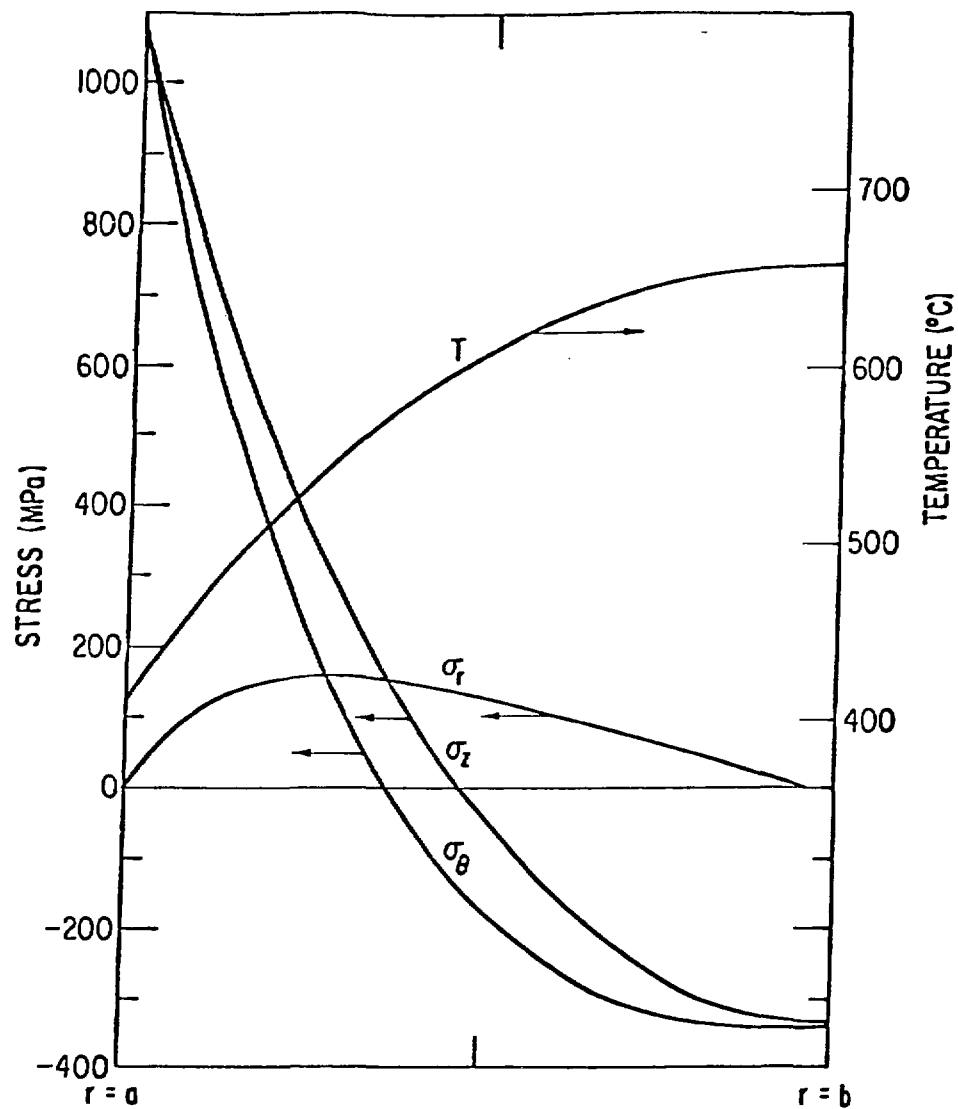


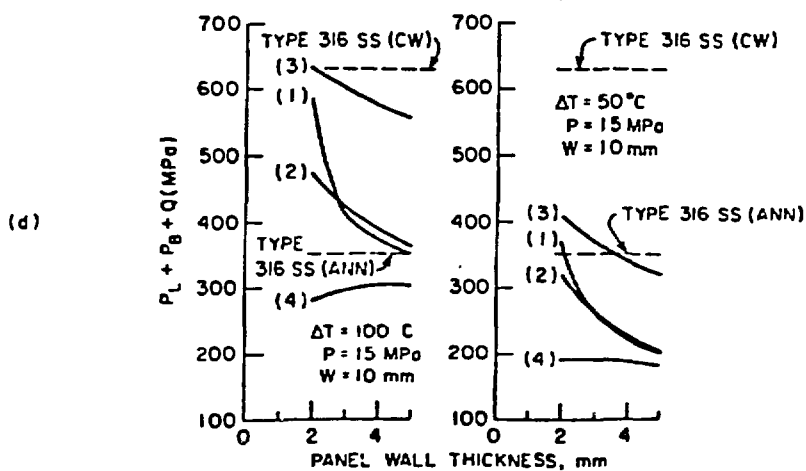
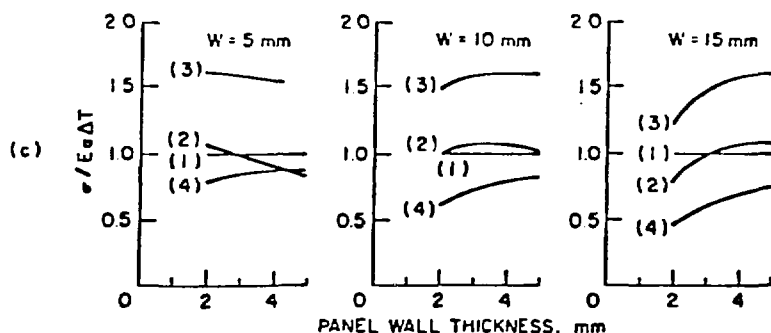
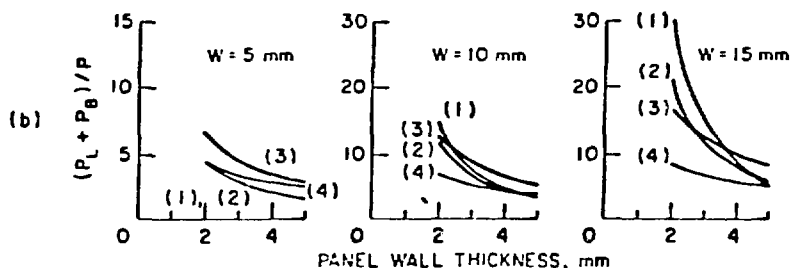
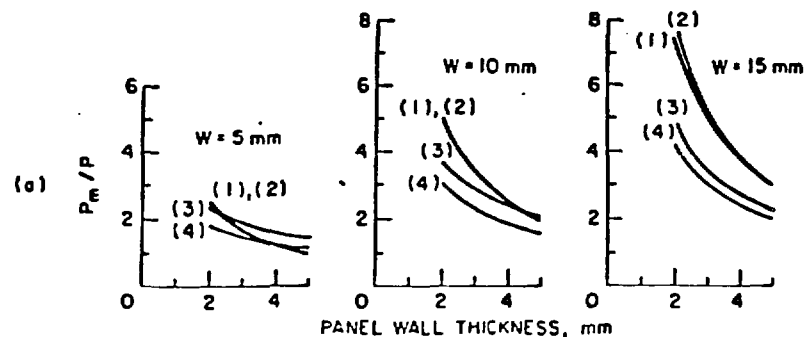
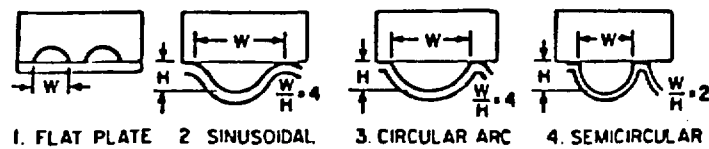


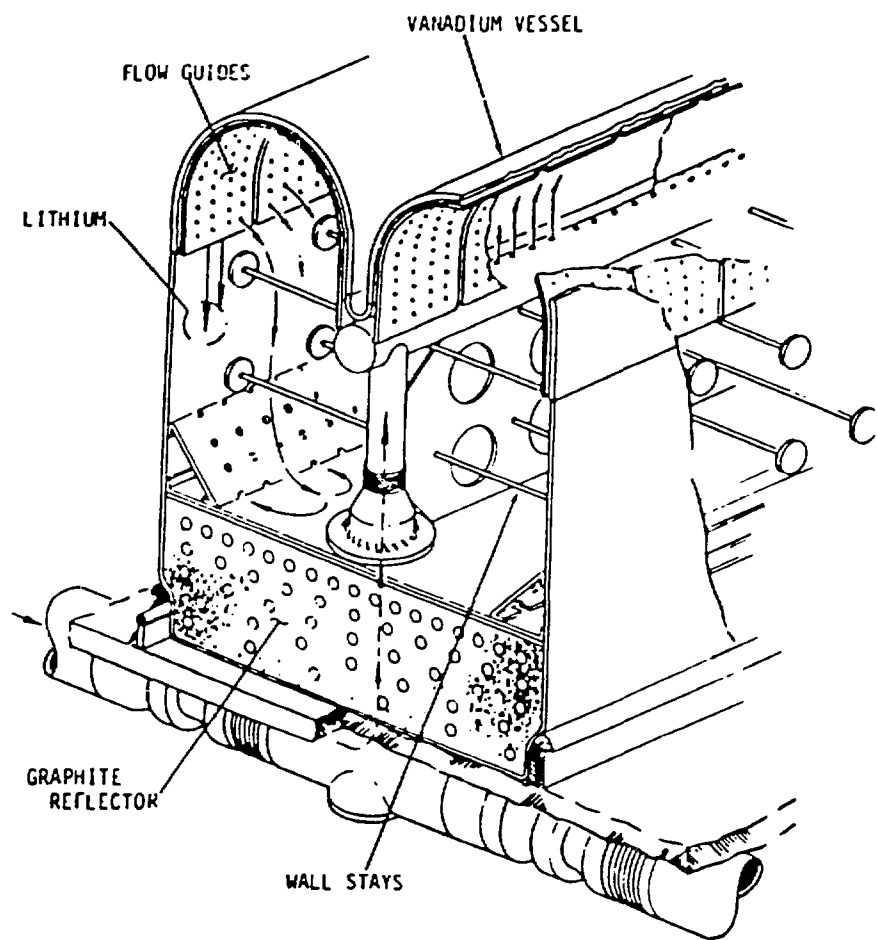
(a)

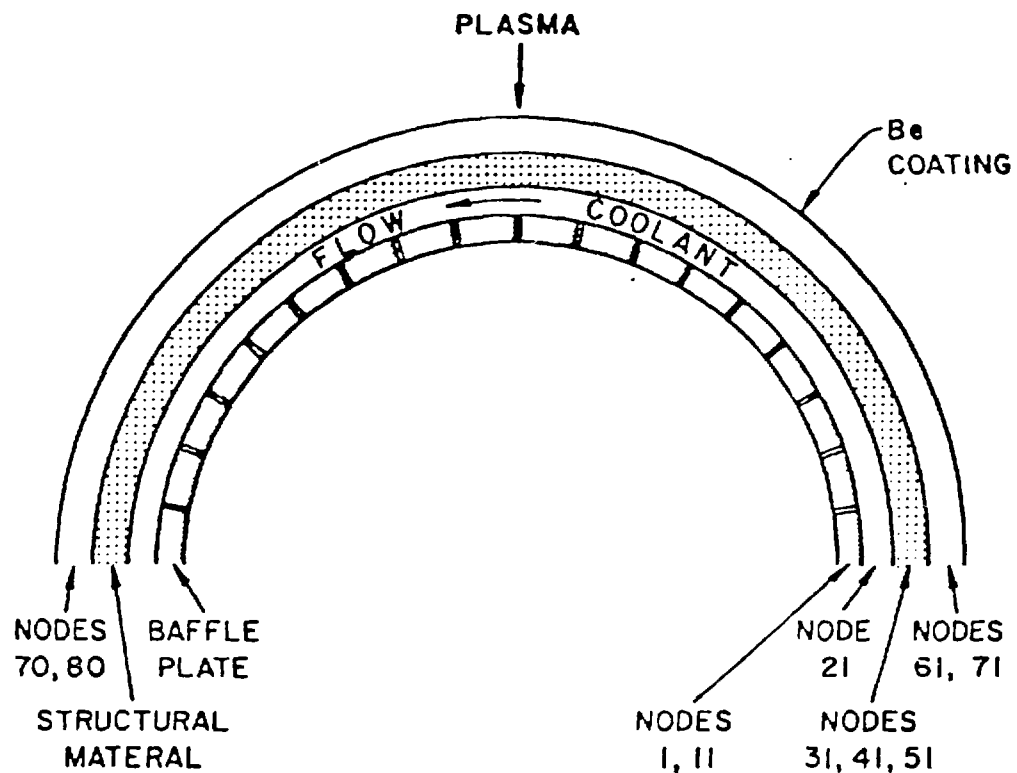
(b)









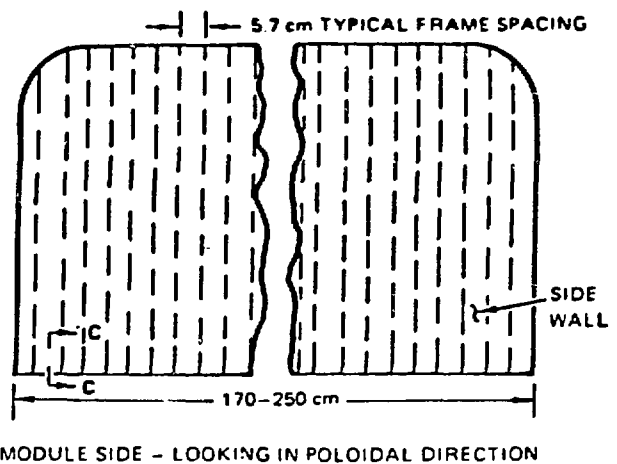
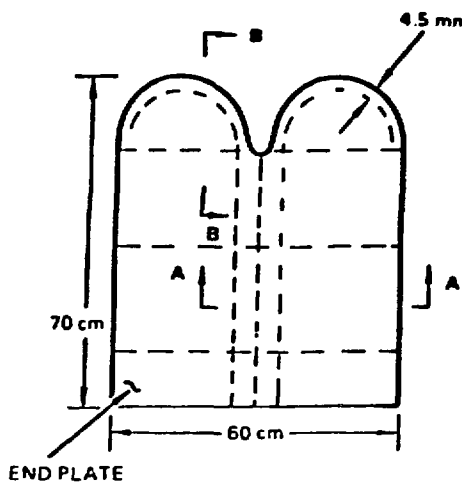


COOLANT NODES 21 - 30 (10)

BAFFLE PLATE NODES 1 - 19 (20)

STRUCTURAL NODES 31 - 51 (30)

COATING NODES 61 - 80 (20)



MODULE SIDE - LOOKING IN TOROIDAL DIRECTION

MODULE SIDE - LOOKING IN POLOIDAL DIRECTION

